

# Thiols as Volatile Corrosion Inhibitors for Top-of-the-Line Corrosion

Z. Belarbi,<sup>‡\*</sup> T.N. Vu,<sup>\*</sup> F. Farelas,<sup>\*</sup> D. Young,<sup>\*</sup> M. Singer,<sup>\*</sup> and S. Nešić<sup>\*</sup>

## ABSTRACT

The effectiveness of hexanethiol, decanethiol, and 11-mercaptoundecanoic acid for CO<sub>2</sub> corrosion inhibition of carbon steel exposed to top-of-the-line conditions has been investigated. Weight loss measurements were used to measure the corrosion rate in the absence and presence of these volatile inhibitor compounds. After the experiments, steel surfaces were characterized by scanning electron microscopy and energy-dispersive x-ray spectroscopy. In addition, surface characterization of adsorbed decanethiol molecules on carbon steel was performed using x-ray photoelectron spectroscopy. The results suggest the formation of an adsorbed inhibitor film on the steel surface, leading to a decrease in corrosion rate. Persistency experiments were also performed to evaluate the residence time for inhibitors adsorbed on carbon steel. Among the inhibitors tested, decanethiol showed very good corrosion inhibition properties as well as high persistency.

**KEY WORDS:** CO<sub>2</sub> corrosion, decanethiol, inhibition, top-of-the-line, x-ray photoelectron spectroscopy

## INTRODUCTION

Top-of-line corrosion (TLC) is a phenomenon of global importance in the oil and gas industry, being problematic for both offshore and onshore fields.<sup>1-3</sup> In stratified flow regimes, conventional CO<sub>2</sub> corrosion inhibitors cannot be used to protect the top of the line because the inhibitors

do not reach the upper surface of the pipe; only the lower surface that is in contact with the liquid phase is effectively protected against corrosion. Therefore, the condensation of water in wet gas flow can result in the development of a highly corrosive environment, leading to failure, release of hydrocarbons, environmental damage, risk to life, and costly repairs for damaged pipelines. To combat TLC, Gunaltun and Belghazi<sup>4</sup> recommended batch treatment, or treatment by continuous injection, with a commercial inhibitor comprising N-methyldiethanolamine in order to neutralize the acidity of the corrosive aqueous medium. Belarbi, et al.,<sup>5</sup> have studied the role of amines in the mitigation of CO<sub>2</sub> TLC. It was found that morpholine and diethylamine did not fully protect the steel specimen exposed to the TLC conditions; they only slightly reduced the pH of the condensed water.<sup>5</sup> Volatile corrosion inhibitors (VCIs) are one of the methods used to manage corrosion. The importance and relevance of VCIs are evidenced by the existence of several patents, as well as recent publication of comprehensive reviews thereof.<sup>6-7</sup> A literature search revealed that alkanethiols have been used as corrosion inhibitors for copper<sup>8</sup> and iron,<sup>9-10</sup> 11-mercaptoundecanoic acid is used as corrosion inhibitor for copper coated by dopamine in 3.5 wt% NaCl.<sup>11</sup> It is also used as a corrosion inhibitor for stainless steel in a phosphate buffer containing 0.16 M NaCl.<sup>12</sup> However, no work has been reported in the literature related to TLC inhibition mechanisms using alkanethiols in conditions that simulate those encountered in the oil and gas industry.

In this paper, research on alkanethiols as novel VCIs is presented. The emphasis in this work was placed

Submitted for publication: January 5, 2017. Revised and accepted: March 1, 2017. Preprint available online: March 2, 2017, <http://dx.doi.org/10.5006/2385>.

<sup>‡</sup> Corresponding author: E-mail: [belarbi@ohio.edu](mailto:belarbi@ohio.edu).

<sup>\*</sup> Institute for Corrosion and Multiphase Technology, Department of Chemical and Biomolecular Engineering, Ohio University, Athens, OH 45701.

on better understanding of the TLC inhibition mechanism by alkanethiols in CO<sub>2</sub> environments, and identifying the type of chemical or physical bonds likely to form between the alkanethiols and the carbon steel surface.

## EXPERIMENTAL PROCEDURES

### Materials and Chemicals

Hexanethiol, decanethiol, and 11-mercaptoundecanoic acid used in this research were acquired from Sigma-Aldrich<sup>†</sup>. Specimens used in the weight loss experiments were made of an API<sup>(1)</sup> 5L X65 carbon steel with a tempered martensite microstructure; its chemical composition is given in Table 1.

### Weight Loss Measurements

The experimental setup used for evaluating the efficacy of VCIs under TLC conditions is shown in Figure 1. Weight loss samples were used to measure the corrosion rate at the top of the line. The bulk aqueous phase comprises 1 wt% NaCl electrolyte, sparged with CO<sub>2</sub> for 2 h to facilitate deoxygenation and ensure saturation. Carbon steel X65 samples (exposed area = 7.917 cm<sup>2</sup>) were mechanically polished using silicon carbide paper (600 grit), cleaned with isopropanol in an ultrasonic bath, and dried at room temperature before introduction into the glass cell. A pH probe was used to measure the pH of the bottom solution before and after adding the VCI. In order to have a gas temperature of 65°C, the bottom solution was heated to 72°C. Two weight loss specimens were flush-mounted at the top of the experimental setup, controlling their temperature at 32°C using a cooling coil. It was assumed that the steel surface got wet immediately after the insertion of the samples which was caused by water condensation that happened as a result of the difference in temperature between the steel sample (~20°C initially) and the water saturated gas phase at 65°C.

Corrosion rate of the specimen at the top (TLC rate) with and without the addition of inhibitors was measured following ASTM<sup>(2)</sup> Standard G1.<sup>13</sup> The detailed TLC experimental matrix for the experimental work is shown in Table 2. The effect of adding inhibitor before or after insertion of specimens was evaluated in the water phase, showing no difference in the final corrosion rate on both procedures. These results will be presented in a future publication.

The average corrosion rate is determined by:

$$CR = (K \times W) / (A \times t \times \rho) \quad (1)$$

<sup>†</sup> Trade name.

<sup>(1)</sup> American Petroleum Institute (API), 1220 L St. NW, Washington, DC 20005.

<sup>(2)</sup> American Society for Testing and Materials (ASTM), 100 Barr Harbor Drive, West Conshohocken, PA 19428-2959.

TABLE 1

Composition (wt%) of API 5L X65 Carbon Steel

Element	C	Nb	Mn	P	S	Ti	V	Ni	Fe
X65	0.05	0.03	1.51	0.004	<0.001	0.01	0.04	0.04	Balance

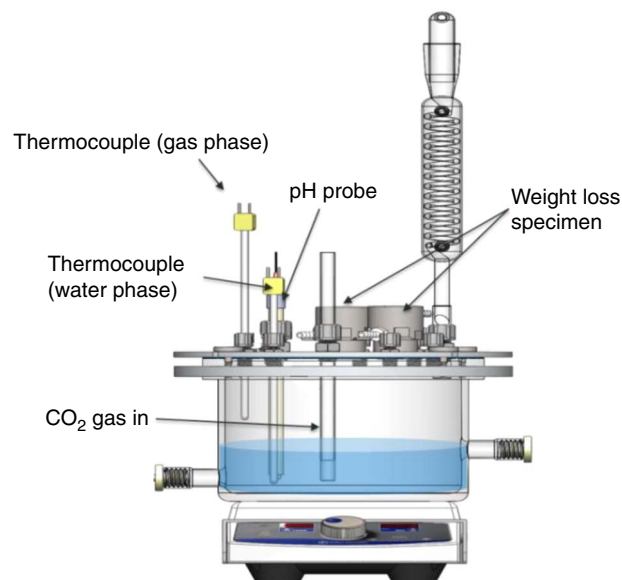


FIGURE 1. Experimental setup for evaluating efficacy of VCI candidates for TLC.

TABLE 2

Test Matrix for TLC Inhibition with Thiols

Total pressure (bar)	1
pCO <sub>2</sub> (Pa)	66 × 10 <sup>3</sup>
Solution	1 wt% NaCl
Solution temperature at the bottom	74 ± 2°C
Gas temperature	65 ± 2°C
Sample temperature	32 ± 2°C
Calculated water condensation rate (mL/m <sup>2</sup> /s)	0.6
Working electrode	X65 carbon steel
Hexanethiol (ppm <sub>v</sub> )	100, 400
Decanethiol (ppm <sub>v</sub> )	100, 400
11-mercaptoundecanoic acid (ppm <sub>v</sub> )	100

where CR: corrosion rate in mm/y; K: conversion factor  $8.76 \times 10^4 = 24 \text{ h/d} \times 365 \text{ d/y} \times 10 \text{ mm/cm}$ ; W: weight loss in g; A: area in cm<sup>2</sup>; t: time of exposure in h; and  $\rho$ : density of steel, 7.87 g/cm<sup>3</sup>.

The residence time experiments for decanethiol and 11-mercaptoundecanoic acid (dilution test) was evaluated by renewing the solution at a flow rate of 1.7 L/min (Figure 2). A borescope was used to observe the condensation process in situ during the dilution test.

### Surface Analysis

Surface analysis of the exposed electrode was performed with a JEOL JSM-6090 LV<sup>†</sup> scanning

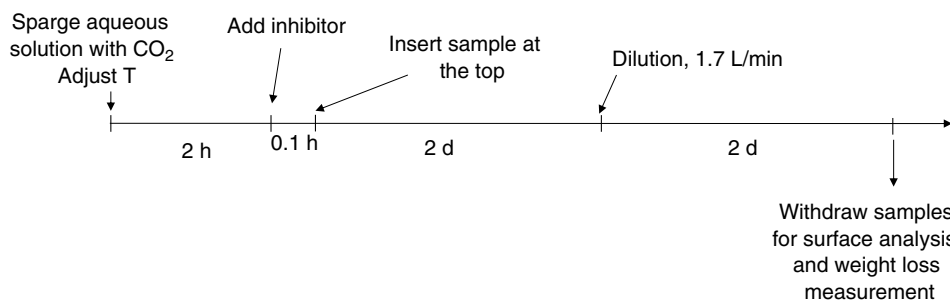


FIGURE 2. Experimental procedure for establishing residence time of thiols.

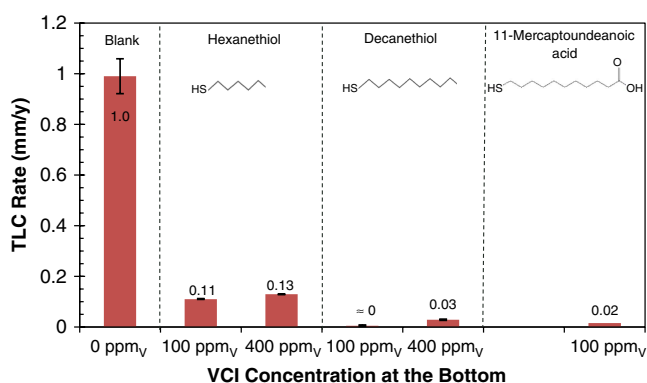


FIGURE 3. Corrosion rate by weight loss measurement of the uninhibited and inhibited TLC specimens (water-condensation rate [WCR] = 0.6 mL/m<sup>2</sup>/s). Note: VCI candidate concentrations on x-axes are the injected concentration for the bottom solution.

electron microscope (SEM) and an EDAX<sup>†</sup> energy dispersive x-ray spectroscopy (EDS) system. Imaging was performed at an accelerating voltage of 15 kV using a secondary electron detector (SEI). The x-ray photoelectron spectroscopy (XPS) analyses were performed with a VG Scientific ESCALAB MKII<sup>†</sup> spectrometer using an Al K $\alpha$  x-ray source (1,486.6 eV). The instrumental resolution was 1.2 eV with a slit width of 0.6 cm. Samples were maintained at ambient temperature (25°C) at a pressure of  $5 \times 10^{-7}$  Pa. The

following XPS regions were recorded: Fe2p, O1s, C1s, and S2p. In order to verify the reproducibility of results, XPS analysis was done on six different spots on each sample.

## RESULTS AND DISCUSSION

### Efficacy of Thiols as Volatile Corrosion Inhibitors for Top-of-the-Line Corrosion

The TLC rate obtained by weight loss is shown in Figure 3. The results show that under the baseline conditions, the X65 carbon steel specimen was corroded at a TLC rate of 1.0 mm/y and its surface was fully covered by a corrosion product (Figure 4). EDS analysis detected Fe, C, and some alloying elements, which suggested the presence of a residual iron carbide layer.<sup>14</sup> In the presence of hexanethiol, the TLC rate was 10 times lower than the baseline test (0.1 mm/y). Under these conditions, the steel surface was only partially protected. The SEM images and EDS analyses (Figure 5) confirmed this conclusion, showing alternating corroded and protected areas. In the presence of decanethiol and 11-mercaptoundecanoic acid the corrosion rate decreased to reach a value lower than 0.03 mm/y. No corrosion was apparent (Figures 6 and 7), and the grooves resulting from specimen polishing remained clearly visible after 2 d of exposure to TLC conditions. The surface of the carbon steel was fully protected.

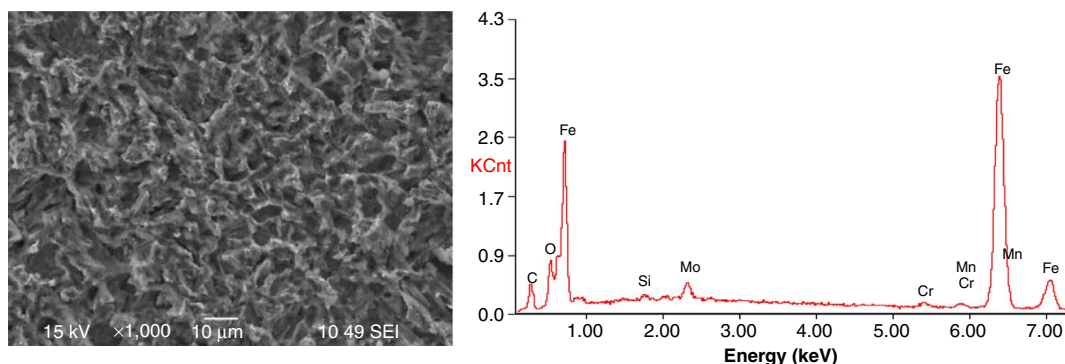


FIGURE 4. SEM image and EDS analysis of the blank sample after 2 d.

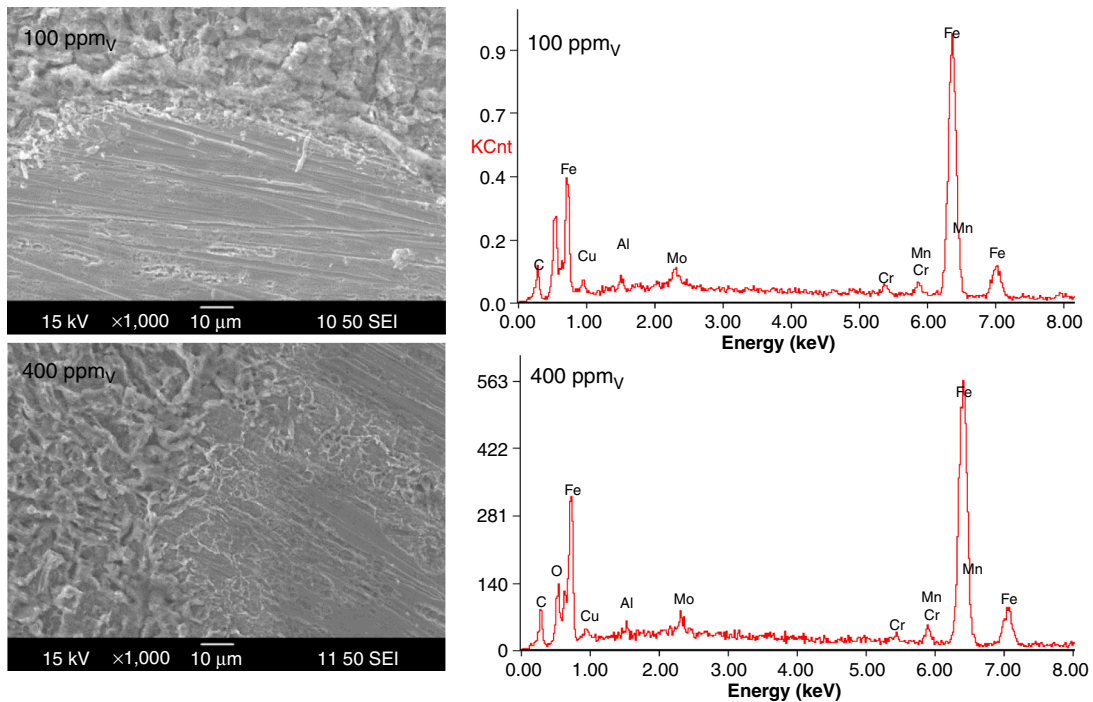


FIGURE 5. SEM images and EDS analysis of the sample in the presence of hexanethiol after 2 d.

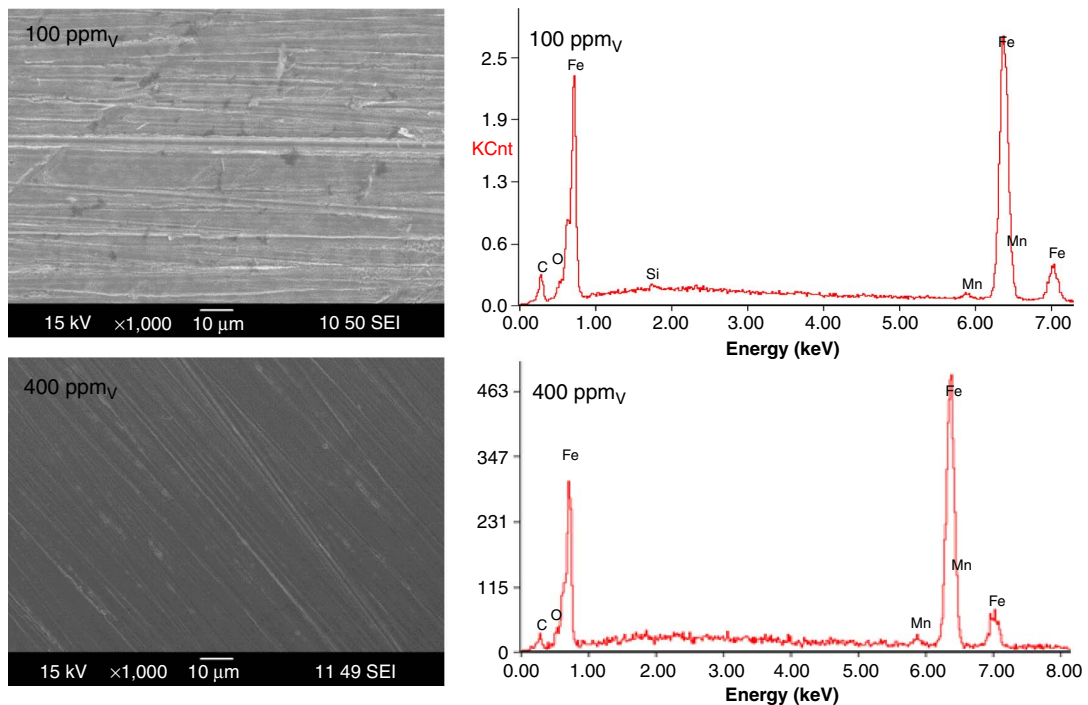


FIGURE 6. SEM images and EDS analysis of the sample in the presence of 100 ppm of decanethiol after 2 d.

*Investigation of the Interaction Between Thiol and the Steel Surface Using X-Ray Photoelectron Spectroscopy*—To further characterize the inhibitor films adsorbed on the steel surface to determine whether they were physisorbed or chemisorbed, XPS analyses were

performed on a freshly polished carbon steel and on carbon steel surfaces after 2 d of exposure to the condensed water in the presence of 400 ppm<sub>v</sub> of decanethiol. Figure 8 shows the XPS spectra of the carbon steel both as freshly polished and exposed to

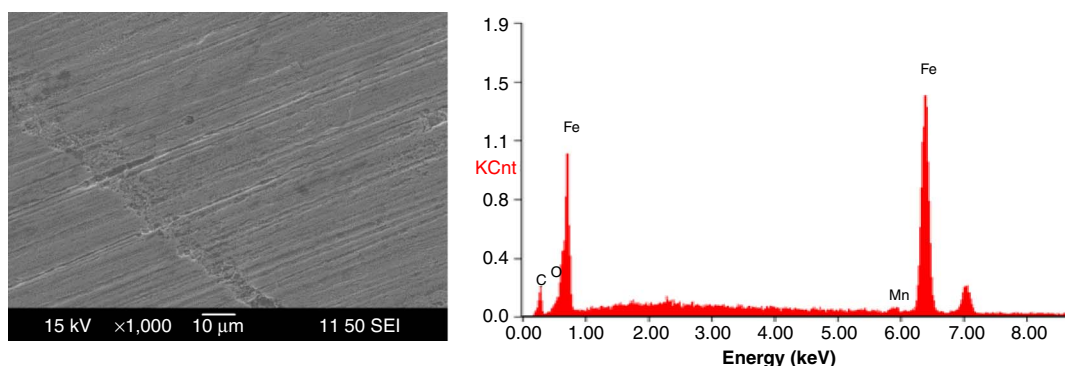


FIGURE 7. SEM images and EDS analysis of the sample in the presence of 11-mercaptoundecanoic acid after 2 d.

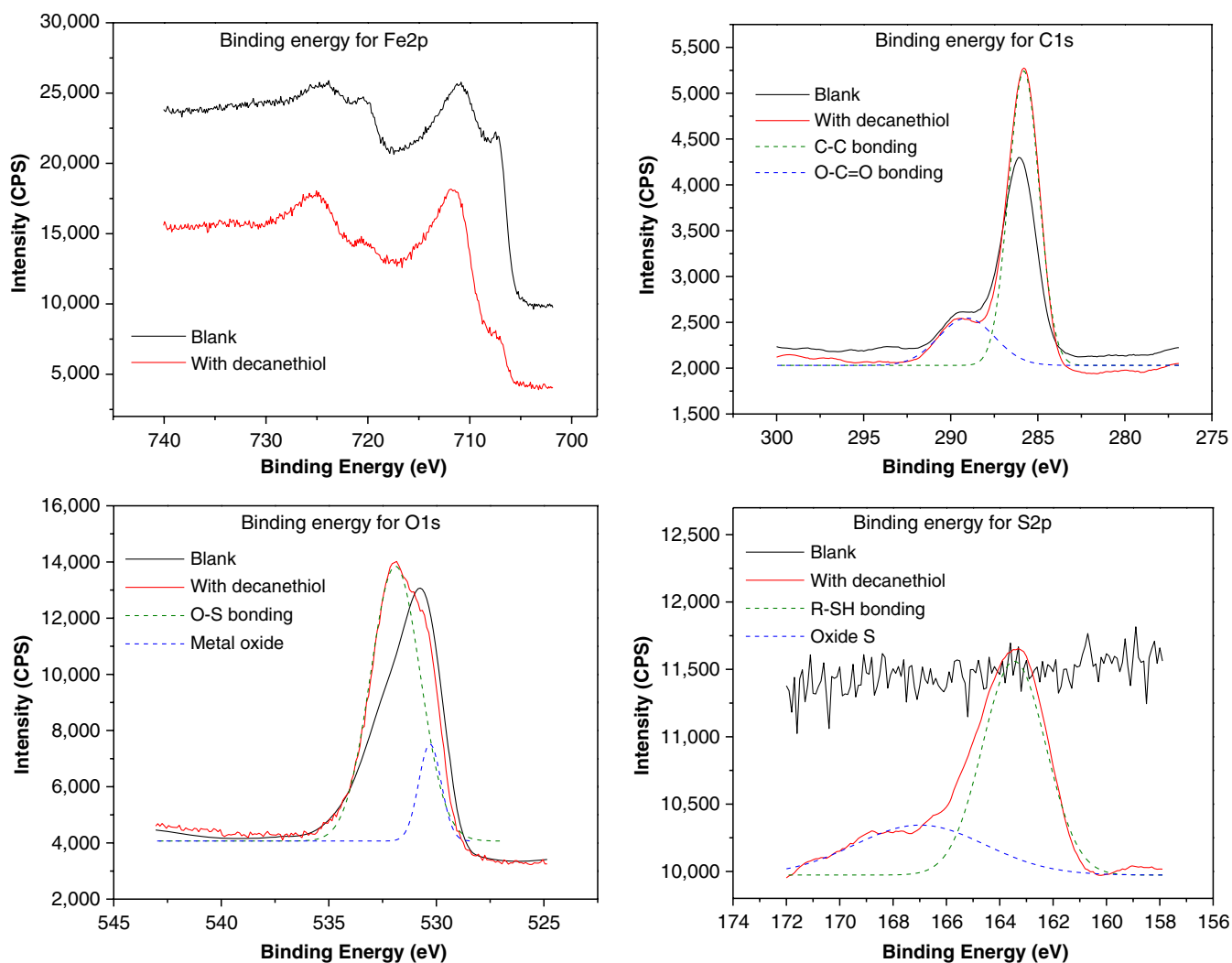


FIGURE 8. XPS spectra of bare steel (blank) and steel electrode exposed to TLC conditions after 2 d in the presence of 400 ppm<sub>v</sub> of decanethiol.

TLC conditions. In the absence and presence of decanethiol, two binding energies of 707.1 eV Fe2p<sub>3/2</sub> and 720.2 eV Fe2p<sub>1/2</sub> were observed. The splitting energy between Fe2p<sub>3/2</sub> and Fe2p<sub>1/2</sub> is equal to 13.1 eV, corresponding to the components of the Fe2p of

metallic iron.<sup>15</sup> The peaks around 710 eV Fe2p<sub>3/2</sub> and 724 eV Fe2p<sub>1/2</sub> correspond to the Fe2p signatures of oxidized iron species;<sup>15</sup> reported literature values<sup>15</sup> have assigned the Fe2p<sub>3/2</sub> peak to Fe<sub>2</sub>O<sub>3</sub> (710.8 eV to 710.9 eV) and Fe<sub>3</sub>O<sub>4</sub> (708.2 eV to 710.4 eV). From the

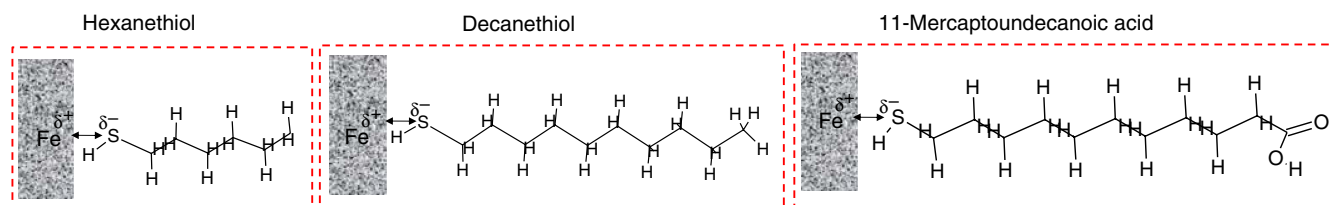


FIGURE 9. Possible interactions between thiols groups and metal surface. (↔): Van der Waals bonding.

shape of the spectra and line positions in Figure 8, it appears that the steel surface is composed of a mixture of metallic and oxidized iron (FeO). The proportions of iron oxides and iron are the same for the bare steel specimen and the steel specimen treated with decanethiol, as suggested by the Fe2p peak positions and intensities. In order to corroborate the presence of oxides on the steel surface the O1s binding energy peak was analyzed. The O1s core level of iron-containing surfaces can be resolved into five components that are located at 530.2 eV (Fe<sub>2</sub>O<sub>3</sub> and Fe<sub>3</sub>O<sub>4</sub>), 531.2 eV for (Fe(OH)<sub>x</sub>), 532.1 eV (H<sub>2</sub>O), 533.1 eV (C-O-C), and 534.4 eV (O=C-O).<sup>15</sup> As already suspected from the analysis of the Fe2p peak, the bare electrode clearly exhibits an FeO component (530.4 eV) and experimental data overlap the fit. In the presence of decanethiol, the overall O1s spectra was deconvoluted into two peaks with binding energies of 530.4 eV and 532 eV, reflecting the presence of an FeO component and oxidized sulfur (S-O) on the steel surface, respectively. Pirlot, et al.,<sup>15</sup> have shown that Fe substrates react with pure n-dodecanethiol, leading to surface modification. Two types of iron substrates, polished and electrochemically reduced, were reacted with pure n-dodecanethiol and characterized by XPS. It was found that the electrochemically reduced surfaces, rich in the less stable Fe(OH)<sub>x</sub> and presenting a lower oxide film thickness, lead to modified surfaces of better quality in terms of possessing a well-controlled interface between the grafted molecule and the iron substrate. The C1s binding energy spectra were composed of two peaks at 286 eV and 289 eV to 290.5 eV. It is common to observe carbon-containing contaminants, such as the peak observed at 286 eV, solely associated with sample handling. This peak is generally used as an energy reference. The intensity of the peak at 286 eV increased in the presence of inhibitor; therefore, the presence of C-C bonding could be related to the inhibitor alkyl tail. The second peak at 289 eV to 290.5 eV (O-C=C) is an artifact. There is no binding energy peak belonging to C1s at 286 eV,<sup>16</sup> meaning no presence of iron carbide at the steel surface. For the bare steel surface, there is no comparable binding energy peak assignable to sulfur in this range. However, the XPS spectrum of the steel electrode exposed to TLC conditions shows obvious binding energy peaks at 164 eV and 169 eV, which are assigned to S2p of the free thiol and oxidized sulfur (sulfate

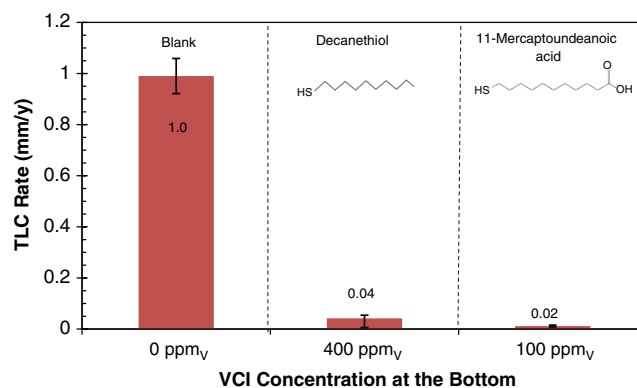


FIGURE 10. Corrosion rate by weight loss measurement of the uninhibited and inhibited TLC specimens (WCR=0.6 mL/m<sup>2</sup>/s). Note: VCI candidate concentrations on x-axes are the injected concentration for the bottom solution.

or sulfite), respectively. There is no binding energy peak belonging to Fe-S at 162.1 eV, meaning no chemisorption of decanethiol on the steel surface.<sup>17</sup> The binding energy peak belonging to oxidized sulfur can be postulated to mean that decanethiol on the steel surface is unstable in air. All of these results support the physisorption of decanethiol on the steel surface. Figure 9 shows the possible interactions between the steel surface, assuming that it is positively charged, and thiols.<sup>18-20</sup> It has been reported in the literature<sup>5</sup> that the steel surface is positively charged in acid environments, based on potential of zero charge measurements; therefore, the adsorption of anions or molecules possessing permanent dipole is considered likely. The chemical structure of thiols plays a significant role and determines their effectiveness as corrosion inhibitors. The inhibiting efficacy of thiols depends on the inductive effect of various functional groups related to the sulfur atom. Evans<sup>21</sup> discussed the influence of substituents on the protective effect of organic inhibitors. The sulfur atom (heteroatom) possesses a free electron pair which can establish Van der Waals secondary bonding interactions with the steel surface (Figure 9). Therefore, thiols can easily desorb because they do not form a primary chemical bond.

*Identification of Residence Time (Persistency Test) of Thiols* — Corrosion rates obtained by weight loss are shown in Figure 10. In the presence of 11-mercaptoundecanoic acid and decanethiol, corrosion rates are very low, 0.04 mm/y for decanethiol

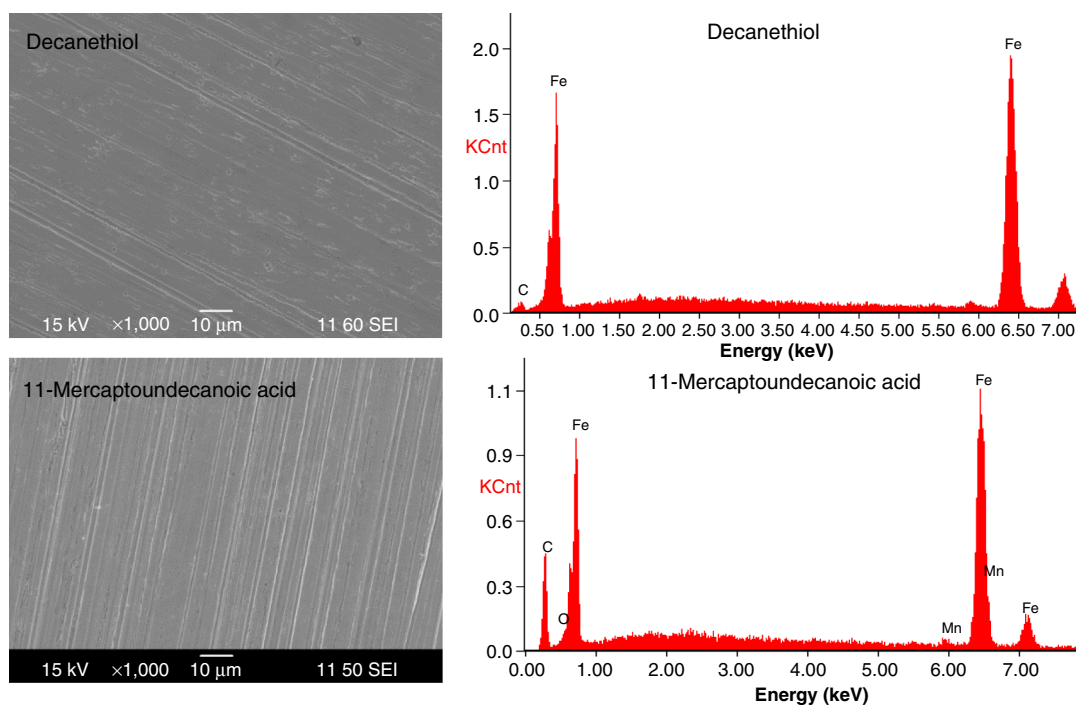


FIGURE 11. SEM images and EDS analysis of the sample in the presence of thiols after dilution test.

and 0.01 mm/y for 11-mercaptoundecanoic acid. The surface of the specimen was fully protected and no corrosion products were observed after 4 d, indicating a good persistency of the tested thiols. The SEM images and EDS analysis of the specimen surface (Figure 11) showed the absence of corrosion products, which was already established from the weight loss measurements. In addition, the SEM images did not show the presence of localized attack. The good persistency of thiols observed in this research could be a result of their low association by hydrogen bonding and their lower solubility in water. Thiol is a sulfur analog of alcohol, but the smaller difference in electronegativity between the sulfur atom and the hydrogen atom makes the S-H bond less polarized than the O-H bond, leading to a diminished propensity to form hydrogen bonds.<sup>22</sup> In other words, “inhibitor/steel” affinity is stronger than for “inhibitor/water.”

## CONCLUSIONS

In this work, the weight loss method was used to study the TLC inhibition mechanism in the presence of hexanethiol, decanethiol, and 11-mercaptoundecanoic acid in a CO<sub>2</sub> environment and acidic pH. The *mechanisms* were investigated by studying their interaction with the steel surface. As a result of this study, the following conclusions were drawn:

❖ With the same added amount (100 ppm<sub>v</sub>), decanethiol and 11-mercaptoundecanoic acid provided a better protection against TLC than hexanethiol.

❖ XPS analysis suggests physisorption of decanethiol on the steel surface as no primary chemical bond formed between metal and sulfur (Fe-S bond) could be identified.

❖ The inhibitor films of decanethiol and 11-mercaptoundecanoic acid are characterized by a high hydrophobicity which provides an excellent barrier against corrosive species from attacking the underlying carbon steel substrate.

## ACKNOWLEDGMENTS

The authors would like to thank the following companies for their financial support: Quadrant Energy, BHP Billiton, BP, Chevron, ConocoPhillips, MI-Swaco, Petronas, PTTEP, Woodside, and Repsol. The authors are grateful to Prof. David Ingram of the “Edwards Accelerator Laboratory—Ohio University” for his help on ex situ XPS experiments. Also, the technical support from the lab’s staff at Institute for Corrosion and Multiphase Technology by Mr. Alexi Barxias, Mr. Cody Shafer, and Mr. Phil Bullington is highly appreciated.

## REFERENCES

1. H. Mansoori, R. Mirzaee, A.H. Mohammadi, F. Esmailzadeh, *Oil Gas J.* 111, 7 (2013): p. 106.
2. H. Mansoori, R. Mirzaee, F. Esmailzadeh, D. Mowla, *Oil Gas J.* 111, 12 (2013): p. 88.
3. H. Mansoori, F. Esmailzadeh, D. Mowla, A.H. Mohammadi, *Oil Gas J.* 111, 6 (2013): p. 64.
4. Y.M. Gunaltun, A. Belghazi, “Control of Top of Line Corrosion by Chemical Treatment,” CORROSION 2001, paper no. 033 (Houston, TX: NACE International, 2001).

5. Z. Belarbi, F. Farel, M. Singer, S. Nestic, *Corrosion* 72, 10 (2016): p. 1300.
6. R. Inzunza, B. Valdez, M. Schorr, *Recent Patents Corros. Sci.* 3 (2013): p. 71.
7. V.S. Saji, *Recent Patents Corros. Sci.* 2 (2010): p. 6.
8. V. Feng, W.K. Teo, K.S. Siow, Z. Gao, K.L. Tan, A.K. Hsieh, *J. Electrochem. Soc.* 144, 1 (1997): p. 55.
9. V. Jovancicevic, Y.S. Ahn, J. Dougherty, B. Alink, "CO<sub>2</sub> Corrosion Inhibition by Sulfur-Containing Organic Compounds," CORROSION 2000, paper no. 007 (Houston, TX: NACE, 2000).
10. T.S.M. Ehteshamzadeh, *Anti-Corros. Meth. Mater.* 53 (2006): p. 147.
11. Y. Chen, S. Chen, Y. Lei, *Corrosion* 68 (2012): p. 747.
12. H. Dadafarin, E. Konkov, S. Omanovic, *Int. J. Electrochem. Sci.* 8 (2013): p. 369.
13. ASTM G1-90, "Standard Practice for Preparing Cleaning and Evaluating Corrosion Test Specimens" (West Conshohocken, PA: ASTM, 1999), p. 15.
14. F. Farel, M. Galicia, B. Brown, S. Nestic, H. Gastaneda, *Corros. Sci.* 52 (2010): p. 509.
15. C. Pirlot, J. Delhalle, J. Pireaux, Z. Mekhalif, *Surf. Coat. Technol.* 138 (2001): p. 166.
16. E. Park, J. Zhang, S. Thomson, O. Ostrovski, R. Howe, *Metall. Mater. Trans. B* 32 (2001): p. 839.
17. H. Zhang, C. Romero, S. Baldelli, *J. Phys. Chem. B* 109 (2005): p. 15520.
18. A. Srhiri, M. Etman, F. Dabosi, *Werkst. Korros.* 43 (1992): p. 406.
19. D. Lavrich, S.M. Wetterer, L.S. Bernasek, G. Scoles, *J. Phys. Chem. B* 102 (1998): p. 3456.
20. M. Hines, J. Todd, P. Guyotsonnest, *Langmuir* 11 (1995): p. 493.
21. U.R. Evans, *The Corrosion and Oxidation of Metals: Second Supplementary Volume* (London, United Kingdom: E. Arnold, 1976), p. 104.
22. M.J. Copley, C.S. Marv, E. Ginsberg, *J. Am. Chem. Soc.* 61, 11 (1939): p. 3161.